Vol. 635: 169–185, 2020
https://doi.org/10.3354/meps13213

MARINE ECOLOGY PROGRESS SERIES
Mar Ecol Prog Ser

Published February 6

Estimating synchronous changes in condition and density in eastern Bering Sea fishes

Arnaud Grüss[1,*], Jin Gao[2], James T. Thorson[3], Christopher N. Rooper[4], Grant Thompson[5], Jennifer L. Boldt[4], Robert Lauth[6]

[1]School of Aquatic and Fishery Sciences, University of Washington, Box 355020, Seattle, WA 98105-5020, USA
[2]Centre for Fisheries Ecosystem Research, Fisheries and Marine Institute of Memorial University of Newfoundland, 155 Ridge Rd, St. John's, NL A1C 5R3, Canada
[3]Habitat and Ecological Process Research Program, Alaska Fisheries Science Center, National Marine Fisheries Service, NOAA, 7600 Sand Point Way NE, Seattle, WA 98115, USA
[4]Fisheries and Oceans Canada, Pacific Biological Station, 3190 Hammond Bay Road, Nanaimo, BC V9T 6N7, Canada
[5]Resource Ecology and Fisheries Management Division, Alaska Fisheries Science Center, National Marine Fisheries Service, NOAA, 7600 Sand Point Way NE, Seattle, WA 98115, USA
[6]Resource Assessment and Conservation Engineering Division, Alaska Fisheries Science Center, National Marine Fisheries Service, NOAA, 7600 Sand Point Way NE, Seattle, WA 98115, USA

ABSTRACT: Estimating fish condition, the relative weight of an individual fish given its body length, is a convenient way to relate the physiological health and energetic status of fishes to their productivity. Despite evidence of density-dependence effects on condition in some species, previous research has not jointly estimated synchronous changes in condition and density operating at fine spatial scales (a few km). Therefore, we developed a spatio-temporal modeling approach that simultaneously estimates correlated variation in density (measured as numbers per area) and condition. We applied our approach to 6 eastern Bering Sea (EBS) groundfish species (4 flatfishes and 2 gadoids) for the period 1992–2016, and estimated correlations in spatial variation (unmeasured variation that is stable over time) and spatio-temporal variation (unmeasured variation that changes between years). Spatial variation in density had a strong significant negative association with spatial variation in condition for 3 flatfishes and a positive association for one gadoid. Spatio-temporal variation in density had a significant association with spatio-temporal variation in condition for one flatfish (negative) and one gadoid (positive). Moreover, for the 6 study species, bottom temperature was identified as an important predictor of both density and condition. The increasing trend in bottom temperatures between 1992 and 2016 was accompanied by an overall increase in the abundance-weighted condition of 5 species. We conclude that forecasts of changes in weight-at-age within some EBS groundfish assessments will require an understanding of both density-dependence and bottom temperature effects on fish condition to better prepare for future climate and exploitation changes.

KEY WORDS: Condition · Le Cren's relative condition index · Density-dependence · Spatio-temporal models · Groundfishes · Eastern Bering Sea · Bottom temperature effects

1. INTRODUCTION

The physiological health of fishes and their energetic status have been intensively studied to understand and predict their productivity (Wuenschel et al. 2019). Some of the most popular measures of physiology and energetic status include the hepatosomatic index, which determines the status of fish energy reserves by assessing liver weight relative to somatic weight, and the gonadosomatic index, which de-

*Corresponding author: gruss.arnaud@gmail.com

scribes fish maturity by evaluating gonad weight relative to somatic weight (e.g. Lambert & Dutil 1997b, Copeland et al. 2008, Pardoe et al. 2008, Pardoe & Marteinsdóttir 2009). Many studies have also examined muscle and liver energy content or estimated the percent dry weight of muscle and liver (e.g. Love 1958, Kjesbu et al. 1991, Lambert & Dutil 1997a,b, Boldt & Haldorson 2004). However, while physiological methods provide valuable information for studying fish productivity, they are typically logistically challenging and usually rely on a limited number of samples (Wuenschel et al. 2019).

Morphological indices of condition, which express fish weight relative to its length, are appealing ways to relate the physiological health and energetic status of fishes to their productivity, because of their nondestructive nature and because they are relatively easy to measure (Nash et al. 2006, Boldt et al. 2015, Wuenschel et al. 2019). Morphological indices of condition (hereafter simply referred to as 'condition indices') are integrated measures of physiology that account for fish behavior and life history as well as environmental and species interactions (Murphy et al. 1990). Condition indices can inform potential survival (e.g. Love 1958, Wilkins 1967, Lambert & Dutil 1997b, Paul & Paul 1999), reproduction (e.g. Kjesbu et al. 1991, Rideout et al. 2000, Dutil et al. 2006, Jørgensen et al. 2006), and recruitment successes (e.g. Kjesbu et al. 1992, Chambers & Leggett 1996, Marteinsdottir & Steinarsson 1998, Marshall & Frank 1999) of fishes. One of the most employed condition indices is Fulton's condition factor, which is the ratio of an individual's weight to the cube of its length (Lambert & Dutil 1997b, Nash et al. 2006). Another widely used and similar condition index is Le Cren's relative condition factor (Le Cren 1958), which defines condition as the residuals of an allometric length–weight relationship and, therefore, does not require the relationship between length and weight to be cubic (Froese 2006, Pardoe et al. 2008, Thorson 2015).

Because condition indices provide rich information on potential fish productivity and can be estimated based on larger sample sizes than physiological indices, they are valuable for stock and habitat assessments. Many stock assessments are age-structured and employ weight-at-age estimates to convert abundances into biomasses, and catches in numbers into catches in biomass. Condition indices can be used to generate time-varying weight-at-age estimates, with the goal to improve the goodness-of-fit of age-structured assessment models to data (Thorson 2015). Also, the results of experiments linking fish condition to natural mortality can be utilized to estimate the proportion of a fish age class that is close to lethal condition in order to then adjust natural-mortality-rates-at-age in age-structured assessment models (Casini et al. 2016). Moreover, variation in the relationship between reproductive potential and subsequent recruitment is typically poorly explained (Barrowman & Myers 1996, Francis 1997). By relating reproductive potential to the variation in weight-at-length of fishes, condition indices can help fisheries analysts produce more reliable recruitment estimates. For example, condition indices can serve to better quantify the number of batches spawned per year and the number of eggs spawned per batch of the different age classes of mature fish in relation to their weight (Marshall & Frank 1999, Fitzhugh et al. 2012), or the rate at which these different age classes skip spawning (Rideout et al. 2005, Jørgensen et al. 2006). Finally, estimates of spatial variation in condition can be employed in habitat assessments. For instance, they can serve to identify areas where the condition of mature individuals is high during the spawning season and which may, therefore, have disproportionate importance for spawning output. These areas may then be given primary consideration in spatial management plans aiming to protect spawners (Lloret et al. 2002, Grüss et al. 2018, 2019a).

Spatio-temporal changes in condition and density may often take place simultaneously. A large local increase in density may result in decreased condition due to increased competition for food (e.g. Boxrucker 1987, Pardoe et al. 2008, Casini et al. 2014, Thorson 2015). However, in some areas, at least over a certain time period, density and condition may respond similarly to local environmental conditions. For instance, increased local temperatures may boost prey abundance while being optimal for the physiological processes of the species of interest, thereby increasing both local density and condition for this species (Boldt et al. 2015). Thus, it appears important to quantify density-dependence in fish condition over space and time, and to determine whether correlations between density and condition are likely to be positive or negative at an annual time scale.

Several factors govern physiological and ecological processes, which in turn govern fish condition and density (Casini et al. 2010, 2011, Thorson 2015). In particular, bottom temperature has been found to influence local density and condition simultaneously in many benthic and demersal fish populations (e.g. Michalsen et al. 1998, Hunt et al. 2008, Boldt et al. 2015, Thorson 2015, Laurel et al. 2016). For example,

the shift from sequential cold years to warm years in the eastern Bering Sea (EBS; see Fig. 1), Alaska, that is responsible for changes in population density distribution in some groundfish species may lead to large changes in spatial overlap with prey, with subsequent effects on groundfish condition (Hunt et al. 2008, Boldt et al. 2015). Specifically, the reduction in the extent of the cold pool (i.e. the area of the EBS with bottom temperatures at or below 2°C) in relatively warm years is accompanied by expansions in the habitat occupied by some groundfish species such as walleye pollock *Gadus chalcogrammus*. These groundfish species can then access the Middle Shelf of the EBS where the cold pool would usually persist. The increase in the area occupied by the groundfish species may allow for better foraging opportunities, thereby improving groundfish condition (Hunt et al. 2008, Boldt et al. 2015).

In recent years, statistical models that account for spatial and spatio-temporal structure at a fine scale (a few kilometers), generally referred to as 'spatio-temporal models', have been increasingly used for informing stock and habitat assessments (Grüss & Thorson 2019, Thorson 2019a). In particular, Thorson (2015) developed the first spatio-temporal model estimating spatio-temporal changes in fish condition, which he applied to California Current groundfishes. This spatio-temporal model was designed to understand how much of the total variation in condition among individuals was explained by covariates (including population density, bottom temperature, and calendar day), temporal variation in condition, spatial variation in condition (i.e. unmeasured variation in condition that is stable over time) and spatio-temporal variation in condition (i.e. unmeasured variation in condition that changes between years). Thorson (2015) found that spatial variation in condition and, to a greater extent, spatio-temporal variation in condition explained a large proportion of total variation among individuals.

Given the importance of quantifying density-dependence in fish condition over space and time highlighted above, in this study we extended the approach of Thorson (2015) by developing the first spatio-temporal model simultaneously estimating spatial and spatio-temporal variation in fish density and Le Cren's relative condition factor (hereafter simply referred to as 'condition'). We applied this spatio-temporal model to 6 EBS groundfish species over the period 1992–2016 to answer the following questions: (1) Are correlations between density and condition statistically significant? (2) Are areas with higher density associated with lower condition (e.g. due to density-dependent competition for food) or greater condition (e.g. because high quality habitat leads to localized concentration of fish while being optimal for fish physiological processes)? We developed alternative spatio-temporal models including or not including bottom temperature effects on density and/or condition, and then selected the most parsimonious model for each groundfish species based on Akaike's information criterion (AIC). Next, we examined correlations between spatial variation in density and spatial variation in condition and between spatio-temporal variation in density and spatio-temporal variation in condition. Finally, we analyzed spatio-temporal changes in density and condition in relation to local bottom temperatures, where relevant.

2. MATERIALS AND METHODS

2.1. Model specifications

Our spatio-temporal model is a multivariate log-normal generalized linear mixed model (GLMM) which simultaneously estimates spatial variation (unmeasured variation that is stable over time) and spatio-temporal variation (unmeasured variation that changes between years) in condition (in units of weight per a power-function of length) and density (in units of numbers per area). If we measured density in biomass, then an increase in condition (greater weight per length) would drive an increase in biomass-density even when the number of fish remains constant, thus resulting in a positive correlation ceteris paribus. To avoid this mechanism generating correlations between density and condition, we measure density in numbers rather than biomass. Our spatio-temporal model is implemented with R package 'VAST' v.3.2.2 released in November 2019 (Thorson 2019a), which is publicly available online (https://github.com/James-Thorson-NOAA/VAST).

Typically, measurements of fish body weight, W, are assumed to be randomly distributed around an expected body weight that is calculated as an allometric function of body length:

$$W = g(w)$$
$$w = \alpha l^{\beta} \quad (1)$$

where α is the condition coefficient; β is the allometric coefficient; g is a probability distribution that represents unexplained variation in fish body length; and w is predicted body weight (in units kilograms) for a given length l (in units meters). Le Cren's relative con-

dition factor is calculated from the residuals of this allometric relationship (Le Cren 1958). From weight and length data, our spatio-temporal model approximates condition using a log link function and linear predictors, including a Gaussian Markov random field representing spatial variation in condition and another Gaussian Markov random field representing spatio-temporal variation in condition:

$$\log\left[w\left(s_i,t_i\right)\right] = \delta_w\left(t_i\right) + \omega_w\left(s_i\right) + \varepsilon_w\left(s_i,t_i\right) + \sum_{k=1}^{n_k}\gamma_w\left(t_i,k\right)X\left(s_i,t_i,k\right) + \beta\log\left(l_i\right) \quad (2)$$

where t_i and s_i are, respectively, the year and the location associated with sample i; $\delta_w(t_i)$ is the intercept for year t_i, which is estimated as a fixed effect; $\omega_w(s_i)$ represents spatial variation in condition and is estimated as a random effect; $\varepsilon_w(s_i,t_i)$ represents spatio-temporal variation in condition and is estimated as a random effect; $X(s_i,t_i,k)$ is an array of n_k measured covariates that explain variation for year t_i and location s_i; and $\gamma_w(t_i,k)$ is the estimated impact of covariates. Eq. (2) corresponds to Le Cren (1958)'s condition factor equation:

$$\text{Median}(W) = w(s,t) = \exp\left\{\delta_w\left(t\right) + \omega_w\left(s\right) + \varepsilon_w\left(s,t\right) + \sum_{k=1}^{n_k}\gamma_w\left(t,k\right)X\left(s,t,k\right)\right\} l^{\beta} \quad (3)$$

such that the intercept $\alpha(s,t) = \exp\left\{\delta_w(t) + \omega_w(s) + \varepsilon_w(s,t) + \sum_{k=1}^{n_k}\gamma_w(t,k)X(s,t,k)\right\}$ varies across space and time.

When explaining variation in density (numbers per unit area), we fit a spatio-temporal model to catch data c_i and use a delta-lognormal distribution where the probability of encounter of the species under consideration, p, and its expected density given encounter (referred to as 'positive catch rate'), r, are estimated; these 2 quantities are then multiplied together to yield density estimates (Lo et al. 1992, Grüss et al. 2019b). The delta-lognormal model calculates the probability of catch rate data as:

$$\Pr\left[c\left(i\right) = C\right] = \begin{cases} 1 - p\left(i\right) & \text{if } C = 0 \\ p\left(i\right) \times g\left(C \mid r\left(i\right), \sigma_r^2\right) & \text{if } C > 0 \end{cases} \quad (4)$$

where probability of encounter, $p(i) = 1 - \exp[-a_i\, n(s_i,t_i)]$, follows a Poisson distribution with intensity equal to the product of local group-densities $n(s_i,t_i)$ and the area sampled a_i, under the assumption that the spatial distribution of aggregations in the neighborhood of sampling is random (Thorson 2018); positive catch rate can be re-expressed as $r(i) = u a_i\, n(s_i,t_i)/p(i)$, where u is the expected numbers-per-group, which is used to convert between $a_i n(s_i,t_i)$ (the expected number of independently distributed groups or patches) and $r(i)$ (the expected number encountered); $g(C \mid r(i),\sigma_r^2)$ is the log-normal probability density function for unexplained variation in $c(i)$; and σ_r^2 is residual catch rate variation. Our model approximates local density $n(s_i,t_i)$ similarly to the way it approximates condition:

$$\log\left[n\left(s_i,t_i\right)\right] = \delta_n\left(t_i\right) + \omega_n\left(s_i\right) + \varepsilon_n\left(s_i,t_i\right) + \sum_{k=1}^{n_k}\gamma_n\left(t_i,k\right)X\left(s_i,t_i,k\right) \quad (5)$$

We now generalize these 2 separate models for condition (Eqs. 1–3) and density (Eqs. 4 & 5) to explain how we can simultaneously estimate both, including their correlation. In effect, our model is provided with both catch rate data and weight and length data, in order to simultaneously approximate 2 categories of variables: density (category $c = 1$) and condition ($c = 2$):

$$\log\left[y\left(s_i,t_i\right)\right] = \delta_{c_i}\left(t_i\right) + \sum_{f=1}^{2}L_{c_i,f}^{(\omega)}\omega_f\left(s_i\right) + \sum_{f=1}^{2}L_{c_i,f}^{(\varepsilon)}\varepsilon_f\left(s_i,t_i\right) + \sum_{k=1}^{n_k}\gamma_{c_i}\left(t_i,k\right)X\left(s_i,t_i,k\right) + \beta\log\left(l_i\right) \quad (6)$$

where $y(s_i,t_i) = n(s_i,t_i)$ and $l_i = 0$ when $c_i = 1$, and $y(s_i,t_i) = w(s_i,t_i)$ when $c_i = 2$; 2 'factors' for spatial variation ω_f and the associations (i.e. correlations) $L_{c,f}^{(\omega)}$ of condition and density with each factor are estimated; and 2 other 'factors' for spatial variation ε_f and the associations $L_{c,f}^{(\varepsilon)}$ of condition and density with each factor are also estimated. The matrices $L_{c,f}^{(\omega)}$ and $L_{c,f}^{(\varepsilon)}$ can serve to calculate correlations between spatial variation in density and spatial variation in condition and between spatio-temporal variation in density and spatio-temporal variation in condition, respectively (Thorson et al. 2016). Thus, the settings of our spatio-temporal model fitted to both catch rate data and weight and length data allow one to determine whether some areas with higher density are associated with lower or greater condition. Note that, in a mixed-effects regression, the fixed effects (including the effects of covariates on density and condition in our case) are estimated first, while random effects (including, in our case, correlations between spatial variation in density and spatial variation in condition and correlations between spatio-temporal variation in density and spatio-temporal variation in condition) model the residuals after accounting for the fixed effects. Therefore, our spatio-temporal model first accounts for the effects of covariates on density and condition, and then models density dependence after having accounted for the covariate effects.

More precisely, the spatial variation terms are modeled as Gaussian Markov random fields with correlations over 2 spatial dimensions and among density and condition (Thorson & Barnett 2017):

$$\mathrm{vec}(\boldsymbol{\Omega}) \sim GRF(0, \mathbf{R} \otimes \mathbf{V}_{\omega}) \quad (7)$$

where $\boldsymbol{\Omega}$ is a matrix composed of $\omega_f(s)$ at every location and category of variables (density and condition); $\mathbf{R}$ is a matrix of correlations among locations s, which is calculated from a Matérn function given an estimated decorrelation rate and a transformation matrix representing geometric anisotropy (Thorson et al. 2015); $\otimes$ is the Kronecker product; and $\mathbf{V}_{\omega}$ is the correlation among density and condition:

$$\mathbf{V}_{\omega} = \mathbf{L}_{\omega}\mathbf{L}_{\omega}^{T} \quad (8)$$

where $\mathbf{L}_{\omega}^{T}$ is the transpose of $\mathbf{L}_{\omega}$. Spatio-temporal variation terms are fit independently to each year and are modeled as Gaussian Markov random fields with Matérn covariance, similarly to spatial variation terms (Thorson & Barnett 2017).

2.2. Parameter estimation

All fixed effects of the spatio-temporal model are estimated, by identifying the parameter values that maximize the marginal log-likelihood, in the R statistical platform (R Core Development Team 2019). The Laplace approximation implemented by R package 'TMB' (Kristensen et al. 2016) is employed to compute the marginal log-likelihood through an approximation of the integral across all random effects. TMB uses automatic differentiation to efficiently compute the matrix of second derivatives (which the Laplace approximation employs) and the gradient of the Laplace approximation (which is employed when the fixed effects are maximized). By maximizing the marginal log-likelihood given fixed effects' maximum likelihood estimates, TMB estimates all random effects. In addition, the likelihood of random effects is approximated using the stochastic partial differential equation method (Lindgren et al. 2011), for computational efficiency. Moreover, VAST employs the generalized delta method implemented in TMB to calculate the standard errors of all the fixed and random effects, as well as the standard errors of the derived quantities (Kass & Steffey 1989). We confirm that the spatio-temporal model is converged by checking that the gradient of the marginal log-likelihood is less than 0.0001 for all fixed effects, and that the Hessian matrix of second derivatives of the negative log-likelihood is positive definite.

2.3. Application

We applied our spatio-temporal modeling approach to 6 groundfish species of the EBS (Fig. 1), including 4 flatfish species (Kamchatka flounder *Atheresthes evermanni*, arrowtooth flounder *Atheresthes stomias*, flathead sole *Hippoglossoides elassodon*, and yellowfin sole *Limanda aspera*), and 2 gadoids (Pacific cod *Gadus macrocephalus* and walleye pollock). These 6 species are among the species most frequently encountered by fisheries-independent monitoring programs in the EBS region (Stevenson & Hoff 2009). Moreover, walleye pollock is one of the most abundant and socio-economically important fish predators of the North Pacific region (Aydin & Mueter 2007), with an annual harvestable biomass of ca. 5 million metric tons (mt) and an annual harvested biomass greater than 1.2 million mt (Ianelli et al. 2011, 2014). In spite of its relatively small harvested biomass, arrowtooth flounder is also a key species of the EBS, because of its large predatory impacts on commercially important fish species, particularly walleye pollock (Hunsicker et al. 2013, Livingston et al. 2017).

We used the catch rate (in numbers km^{-2}), total weight (in grams), length (in millimeters), and bottom temperature (in °C; see Fig. S1 in the Supplement at www.int-res.com/articles/suppl/m635p169_supp.pdf) data collected over the period 1992–2016 during the

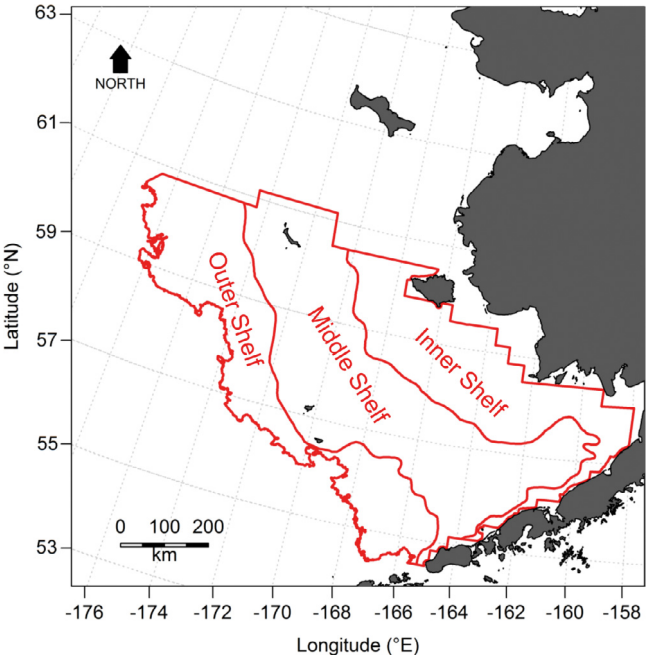

Fig. 1. Inner, Middle and Outer Shelf of the eastern Bering Sea off Alaska

Table 1. Study species and years for which both density and length–weight data are available for these species

Species	Years of data availability
Kamchatka flounder *Atheresthes evermanni*	1995–1997, 2002, 2012–2016
Arrowtooth flounder *Atheresthes stomias*	1996, 2002, 2004–2006, 2008–2012, 2014–2016
Flathead sole *Hippoglossoides elassodon*	1997, 1999–2016
Yellowfin sole *Limanda aspera*	1994, 1999–2016
Pacific cod *Gadus macrocephalus*	1993, 1998–2016
Walleye pollock *Gadus chalcogrammus*	1999–2016

standardized EBS bottom trawl surveys conducted by NOAA's National Marine Fisheries Service Alaska Fisheries Science Center (Stauffer 2004, Lauth & Conner 2016). These surveys are carried out annually in June–July, employ a fixed-station sampling scheme each year involving approximately 376 stations on a 20 × 20 km grid (including areas with more dense sampling near significant islands), and sample monitoring stations using a standard trawl net (83-112 eastern otter trawl) for a targeted on-bottom time of 30 min at a speed of 1.54 m s^{-1}. Individual length and weight data are not consistently collected during these surveys; therefore, for each study species, we did not have length and weight data in some years (Table 1).

For the application, we use a 'predictive process' modeling framework, wherein we define all spatial and spatio-temporal variation terms over a fixed spatial domain Ω using linear interpolation between their values at a specified number of 'knots'. To approximate all the spatial and spatio-temporal variation terms defined over domain Ω, we specify 50 knots uniformly distributed over the 20 × 20 km spatial grid for the EBS, while confirming that our results are qualitatively similar when using more knots. The values of all spatial and spatio-temporal variation terms are tracked at each knot by the spatio-temporal models (Shelton et al. 2014), and the value of a spatial or spatio-temporal variation term at a given location $s \in \Omega$ is interpolated from the value of 3 knots surrounding that location. After having been determined, the locations of the 50 knots is held fixed during model parameter estimation.

To be able to interpolate spatial and spatio-temporal variation from knots to the location of samples and extrapolation grid cells and produce smooth fine-scale maps, we employ a new 'fine-scale' option available in VAST v.3.2.2 (Thorson 2019c), which follows standard practices of software R-INLA (Lindgren 2012, Lindgren & Rue 2015). This new option allows one to interpolate the predictions of spatio-temporal models from knots j to extrapolation grid cells g, using the triangulated mesh constructed from knots (Lindgren 2012, Lindgren & Rue 2015). Specifically, a matrix $\mathbf{M}_g$ with n_g rows and n_j columns is employed, where each row g has value zero except for 3 cells that represent the vertices of the triangle containing extrapolation grid cell g. For example, with the fine-scale option, a vector $\boldsymbol{\omega}_f^*$ at all extrapolation grid cells is predicted from values of $\boldsymbol{\omega}_f$ at all n_j knots:

$$\boldsymbol{\omega}_f^* = \mathbf{M}_g \boldsymbol{\omega}_f \quad (9)$$

where vector $\boldsymbol{\omega}_f^*$ has length and n_g contains the predicted value $\boldsymbol{\omega}_f^*(g)$ for spatial variation for every extrapolation grid cell g (Thorson 2019c).

The spatial scales modeled for the EBS (a few kilometers) are the spatial scales at which density-dependence and other ecological interactions are expected to operate for the 6 study species. All of our study species undertake ontogenetic habitat shifts (typically migrate to establish their normal residence areas offshore and into deeper waters with age) and they all have limited home ranges within their normal residence areas (Witherell 2000, Laman et al. 2018). For example, arrowtooth flounder are found throughout the EBS shelf until age 4, after which they migrate to deeper areas to occupy both the shelf and the slope of the EBS; all arrowtooth flounder life stages maintain relatively small home ranges within their normal residence areas (Witherell 2000).

For each study species, we fit 4 alternative spatio-temporal models: (1) a model without bottom temperature effects; (2) a model with bottom temperature effects on both density and condition; (3) a model with bottom temperature effects on density only; and (4) a model with bottom temperature effects on condition only. We then select the most parsimonious of these 4 models based on AIC (Akaike 1974). Bottom temperature effects include the linear effect of bottom temperature (i.e. the effect of T), as well as the quadratic effect of bottom temperature (i.e. the effect of T^2), representing a dome-shaped response of local density and/or condition to local bottom temperatures. We include both linear and quadratic bottom temperature effects in spatio-temporal models to be able to estimate the optimal bottom temperature for population density and fish condition from the AIC-selected models. Specifically, when a negative qua-

drative effect is estimated, the curvature of the relationship between population density or fish condition and bottom temperature is downwards, and it is then possible to determine the optimal bottom temperature for population density or fish condition. Both the T and T^2 covariates are standardized to have a mean of zero and a variance of 1 prior to being used in the spatio-temporal models; this transformation implies that γX (i.e. a covariate times its coefficient) has a standard deviation equal to γ (Thorson 2015). Next, we use the AIC-selected models to analyze correlations between spatial variation (unmeasured variation that is stable over time) in density and spatial variation in condition, and correlations between spatio-temporal variation (unmeasured variation that changes between years) in density and spatio-temporal variation in condition. Then, for each of the 6 study species, we examine spatio-temporal changes in density and in condition, in relation to local bottom temperatures where relevant.

Finally, for each study species, we reconstruct trends in abundance-weighted condition z (in g):

$$z(t) = \sum_{g=1}^{n_g} \left[a_g \times \hat{n}^*(g,t) \right] \times \hat{\alpha}^*(g,t) \quad (10)$$

where a_g is the surface area (in km^2) associated with extrapolation grid cell g; $\hat{n}^*(g,t)$ is the smoothed density estimated for extrapolation grid cell g in year t (in numbers km^{-2}); and $\hat{\alpha}^*(g,t)$ is the smoothed condition estimated for extrapolation grid cell g in year t (in g). Since this is the first time that an abundance-weighted estimate has been generated with R package 'VAST', we also compare our results with a simplified estimator (see Supplement S2 for details and results).

3. RESULTS

We fitted 4 alternative spatio-temporal models for each of the 6 study species (i.e. a total of 24 spatio-temporal models). The AIC-selected model (i.e. most parsimonious model) of all study species included bottom temperature effects on both density and condition (Table 2), in addition to spatial variation in density and condition (i.e. unmeasured variation in density and condition that is stable over time) and spatio-temporal variation in density and condition (i.e. unmeasured variation in density condition that changes between years). For all models, the absolute value of the final gradient of the log-likelihood function at the maximum likelihood estimates was less than 0.0001 for all fixed parameters and the Hessian of the negative log-likelihood function was positive definite. Moreover, plots of the residuals of the AIC-selected models as a function of fish length all showed random patterns (i.e. none of these plots showed U-shaped or inverted U-shaped patterns), which indicates that our analyses were likely not biased by the collection of different length classes in different years and/or sampling locations (Fig. S3).

Table 2. Model selection results using Akaike's information criterion applied to the maximum marginal likelihood for each of the spatio-temporal models fitted in this study

Species	Bottom temperature effects on			
	None	Density and condition	Density only	Condition only
Kamchatka flounder	442.8	0	226.6	211.9
Arrowtooth flounder	398.7	0	508.9	523.9
Flathead sole	383.1	0	12.0	369.9
Yellowfin sole	1256.8	0	398.1	835.0
Pacific cod	1189.2	0	220.1	352.6
Walleye pollock	928.8	0	643.4	284.3

For all study species except flathead sole and walleye pollock, spatial variation in density was negatively correlated with spatial variation in condition (Fig. 2a). The negative correlation coefficient between spatial variation in density and spatial variation in condition of Kamchatka flounder, arrowtooth flounder, and yellowfin sole was significant ($p < 0.001$ for all 3 species, using a 2-sided Wald test for all significance testing of correlations). The positive correlation coefficient between spatial variation in density and spatial variation in condition of walleye pollock was also significant ($p = 0.01$).

The correlation coefficient between spatio-temporal variation in density and spatio-temporal variation in condition was positive for all study species, except for 2 flatfishes: arrowtooth flounder and flathead sole (Fig. 2b). Only 2 of the correlation coefficients between spatio-temporal variation in density and spatio-temporal variation in condition were significant: the negative correlation coefficient for arrowtooth flounder ($p = 0.01$) and the positive correlation coefficient for Pacific cod ($p = 0.04$).

For all study species, the linear and quadratic effects of bottom temperature on density and condition were usually significant (Table 3). The exceptions to this usual pattern were the linear effect of bottom temperature on walleye pollock density, the quadratic effect of bottom temperature on Pacific cod density, and the quadratic effect of bottom temperature on flathead sole condition. For all species, the linear

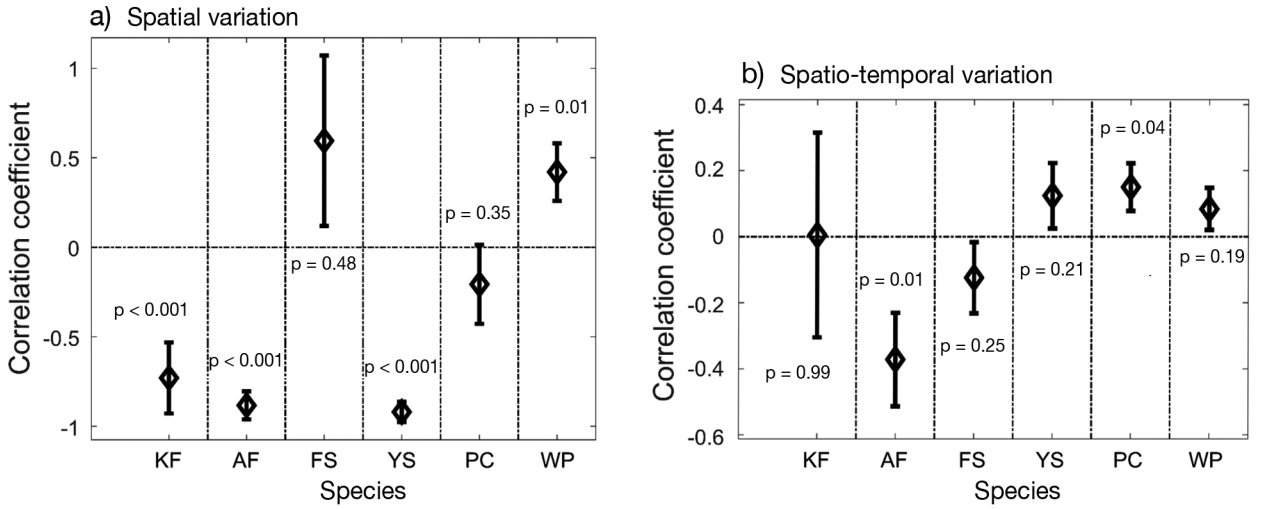

Fig. 2. Mean (±SE) correlation coefficients between spatial variation in density and spatial variation in condition and between spatio-temporal variation in density and spatio-temporal variation in condition, predicted by Akaike's information criterion-selected spatio-temporal models. The p-values are for a 2-sided Wald test (strength-of-evidence measures of importance). KF: Kamchatka flounder *Atheresthes evermanni*; AF: arrowtooth flounder *Atheresthes stomias*; FS: flathead sole *Hippoglossoides elassodon*; YS: yellowfin sole *Limanda aspera*; PC: Pacific cod *Gadus macrocephalus*; WP: walleye pollock *Gadus chalcogrammus*

Table 3. Linear and quadratic bottom temperature effects on density and condition predicted by the Akaike's information criterion-selected spatio-temporal models of the 6 study species, and predicted optimal bottom temperatures for density and condition for the 6 species. The p-values for a 2-sided Wald test (strength-of-evidence measures of importance) are also indicated in parentheses. na: not available

Species	Density			Condition		
	Linear effect	Quadratic effect	Optimal temp. (°C)	Linear effect	Quadratic effect	Optimal temp. (°C)
Kamchatka flounder	0.21 ± 0.03 (p < 0.001)	0.15 ± 0.03 (p < 0.001)	na	14.83 ± 0.79 (p < 0.001)	−8.49 ± 0.72 (p < 0.001)	1.1
Arrowtooth flounder	0.40 ± 0.04 (p < 0.001)	0.12 ± 0.03 (p < 0.001)	na	40.75 ± 0.70 (p < 0.001)	−39.67 ± 1.29 (p < 0.001)	0.5
Flathead sole	0.21 ± 0.03 (p < 0.001)	−0.12 ± 0.02 (p < 0.001)	0.9	0.16 ± 0.06 (p < 0.001)	−0.01 ± 0.03 (p = 0.87)	9.9
Yellowfin sole	0.82 ± 0.05 (p < 0.001)	−0.17 ± 0.04 (p < 0.001)	2.4	6.48 ± 0.21 (p < 0.001)	−1.19 ± 0.08 (p < 0.001)	2.7
Pacific cod	0.16 ± 0.03 (p < 0.001)	−0.002 ± 0.02 (p = 0.91)	9.9	53.36 ± 0.49 (p < 0.001)	−23.13 ± 0.43 (p < 0.001)	1.2
Walleye pollock	0.03 ± 0.03 (p = 0.37)	−0.09 ± 0.02 (p < 0.001)	0.2	11.00 ± 0.58 (p < 0.001)	−3.57 ± 0.36 (p < 0.001)	1.5

effects of bottom temperature on density and condition were positive, while the quadratic effects were usually negative (except for Kamchatka flounder density and arrowtooth flounder density; Table 3). It was, therefore, usually possible to identify the optimal bottom temperature for population density and fish condition for the 6 study species (Table 3).

We examine here, in detail, the patterns of spatial and spatio-temporal variation in density and condition only for Kamchatka flounder, arrowtooth flounder, yellowfin sole, and walleye pollock for select years (see Figs. 3–6), including 1999 and 2012 which were very cold years, and 2016 which was a very warm year (Fig. S1). All the spatial and spatio-temporal variation estimates of the study species for 1992–2016 for which both catch rate and length–weight data were available are provided in the Supplement (Fig. S4).

The expected density of Kamchatka flounder was highest on the Outer Shelf of the EBS, where the expected condition of the species was lowest (Fig. 3a,b). The expected condition for Kamchatka flounder was

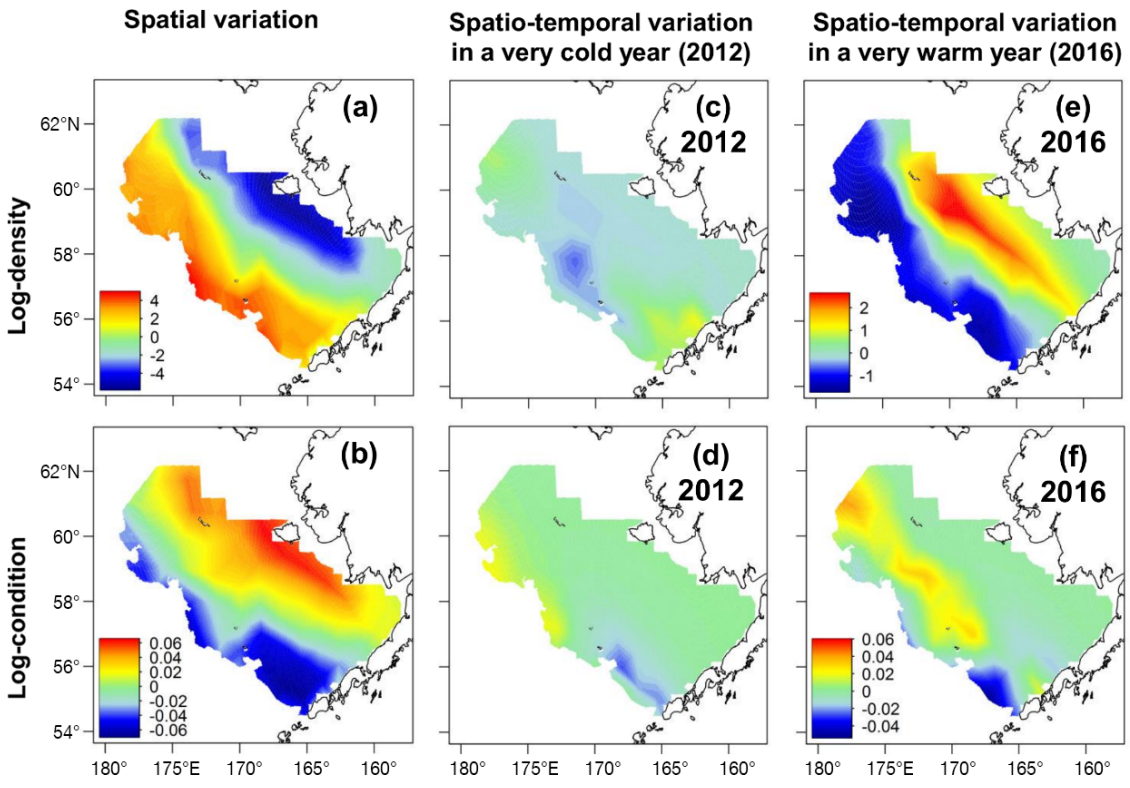

Fig. 3. Spatial variation (i.e. unmeasured variation that is stable over time) in (a) log-density and (b) log-condition, and spatio-temporal variation (i.e. unmeasured variation that changes between years) in (c,e) log-density and (d,f) log-condition for a very cold year (2012) and a very warm year (2016), for the Akaike's information criterion-selected model of Kamchatka flounder *Atheresthes evermanni*. The color legends for spatio-temporal variation in log-density and log-condition are provided in the rightmost column and have units ln(abundance km^{-2}) in the case of log-density and ln(g) in the case of log-condition

highest on the Inner Shelf of the EBS (Fig. 3b). In the very cold year of 2012, arrowtooth flounder density and condition over the entire EBS were lower than their long-term averages (Fig. 4c,d). In the very warm year of 2016, arrowtooth flounder density was higher than its long-term average on the Inner Shelf, where condition was relatively lower than average (Fig. 4e,f). In 2016, arrowtooth flounder condition was higher than its long-term average in the northern and central parts of the Outer Shelf of the EBS (Fig. 4f).

As was the case for Kamchatka flounder, the expected density of arrowtooth flounder was highest on the Outer Shelf of the EBS, where its expected condition was low; the highest values of arrowtooth flounder expected condition occurred on the Inner Shelf of the EBS (Fig. 4a,b). In the very cold year of 2012, arrowtooth flounder density and condition tended to be lower than their long-term averages over the entire EBS, although condition was relatively higher than average in the central part of the Outer Shelf than elsewhere in the EBS region (Fig. 4c,d). In the very warm year of 2016, arrowtooth flounder density was higher than its long-term average on the Inner Shelf, where the condition of the species was lower than average (Fig. 4e,f). In 2016, arrowtooth flounder condition was higher than its long-term average in the northern and central parts of the Outer Shelf of the EBS (Fig. 4f).

The expected density of yellowfin sole was highest on the Inner and Middle Shelf, where the expected condition of the species was lowest (Fig. 5a,b). The highest values of yellowfin sole expected condition were found in the southern part of the Outer Shelf of the EBS (Fig. 5b). In the very cold year of 1999, yellowfin sole density was higher than its long-term average in the northernmost areas of the EBS, contrasting with the rest of the EBS region where the density of the species tended to be lower than average (Fig. 5c,d). In 1999, yellowfin condition was lower than its long-term average on the Inner Shelf (Fig. 5d). In the very warm year of 2016, yellowfin sole density was higher than its long-term average in the southern part of the Outer Shelf, while the condition of the species was higher than average on the Inner Shelf and in the northern part of the Middle Shelf (Fig. 5e,f).

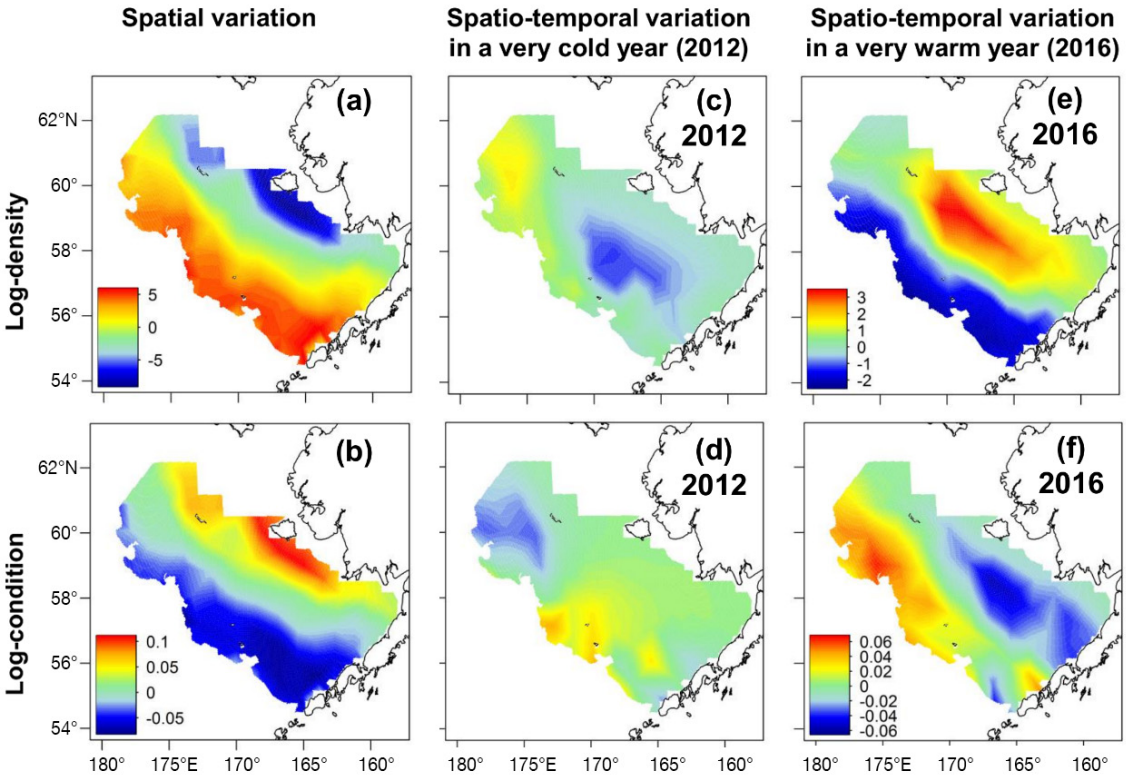

Fig. 4. Description as in Fig. 3, but for arrowtooth flounder *Atheresthes stomias*

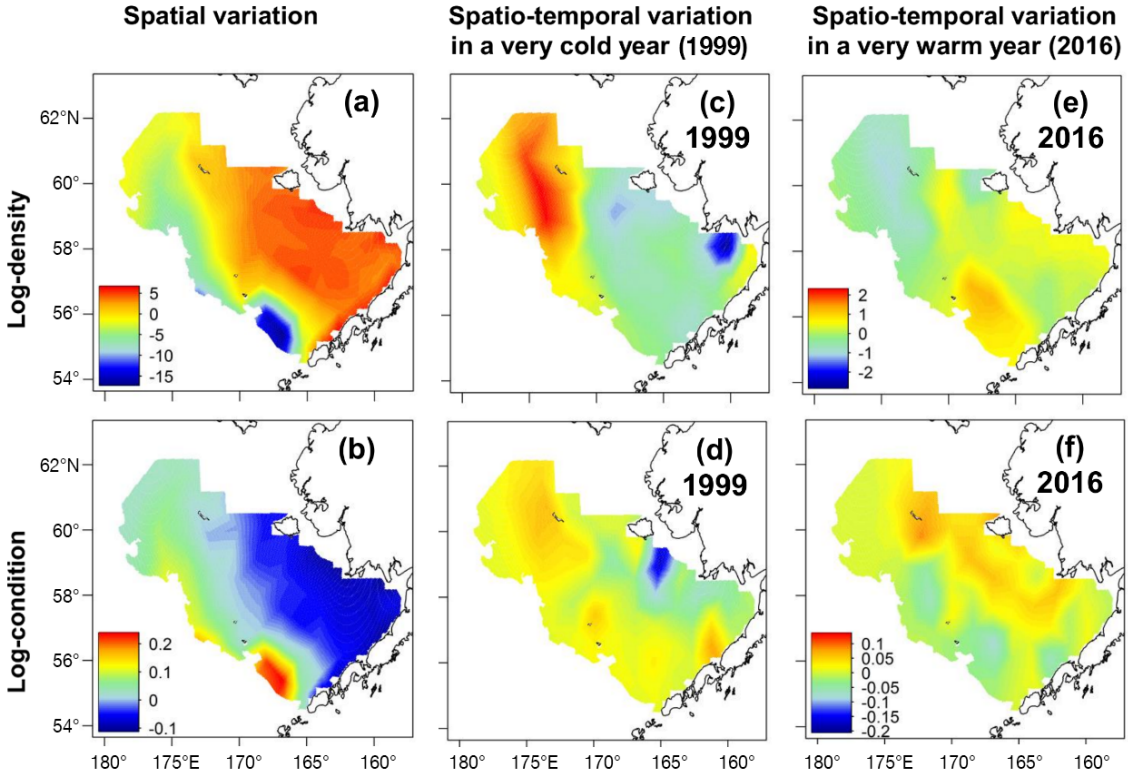

Fig. 5. Description as in Fig. 3, but for yellowfin sole *Limanda aspera* and with 1999 as the very cold year

The expected density of walleye pollock was high on the Middle and Outer Shelves of the EBS, while the greatest values for walleye pollock condition were found on the Outer Shelf (Fig. 6a,b). In the very cold year of 1999, both walleye pollock density and condition were highest in the northern and central parts of the Outer Shelf, and condition was also high in the central part of the Inner Shelf (Fig. 6c,d). In the very warm year of 2016, the density of walleye pollock was greatest on the Inner Shelf, while the largest values for the condition of the species occurred on the Middle Shelf (Fig. 6e,f).

Because the spatio-temporal models estimated near-exact opposite patterns of spatial variation in density and spatial variation in condition for Kamchatka flounder, arrowtooth flounder, and yellowfin sole (Figs. 3–5), we conducted additional analyses to determine whether estimating density and condition jointly (i.e. assuming a correlation between the 2 variables) versus separately (i.e. not assuming a correlation) would yield different results (Fig. S5). For flathead sole, Pacific cod, and walleye pollock, the patterns of spatial variation in condition were virtually unchanged when density and condition were estimated jointly versus separately. By contrast, for Kamchatka flounder, arrowtooth flounder, and yellowfin sole, the spatio-temporal model estimating density and condition jointly shrank spatial variation in condition somewhat towards the inverse of the spatial variation in density, yet patterns of spatial variation in condition were qualitatively similar with or without modeling correlation between density and condition (Fig. S5).

None of the time series of abundance-weighted condition showed a continuous increasing or decreasing trend, except that of Kamchatka flounder (Fig. 7). The time series of abundance-weighted condition of Kamchatka flounder demonstrated a marked increasing trend between 1992 and 2016. Moreover, the abundance-weighted condition of arrowtooth flounder increased between 1992 and 2005 and tended to decrease afterwards. By contrast, the abundance-weighted condition of walleye pollock decreased between 1992 and 2009 and largely increased afterwards. Comparing the first year of the time series and the last year of the time series, the abundance-weighted condition of 5 species (Kamchatka flounder, arrowtooth flounder, flathead sole, Pacific cod, and walleye pollock) increased while that of yellowfin sole showed virtually no change. In the very cold year of 1999 (the coldest year of the period 1992–2016; Fig. S1), the abundance-weighted condition of 4 flat-

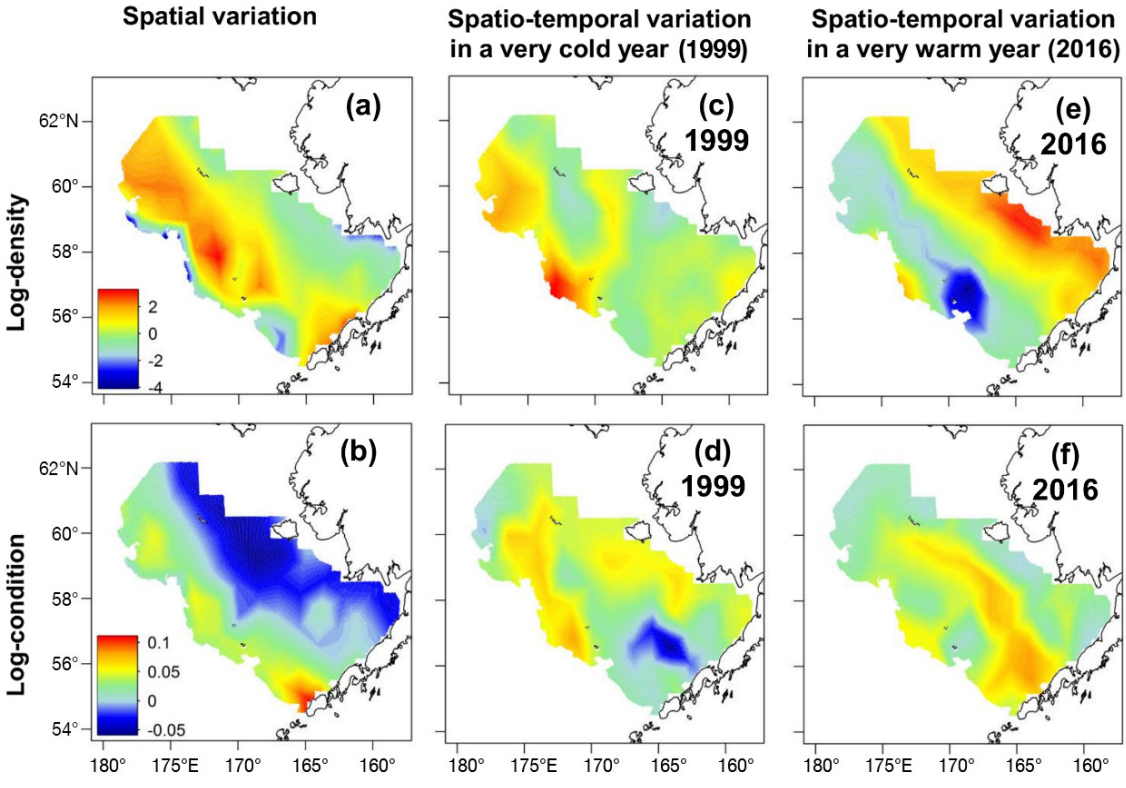

Fig. 6. Description as in Fig. 3, but walleye pollock *Gadus chalcogrammus* and with 1999 as the very cold year

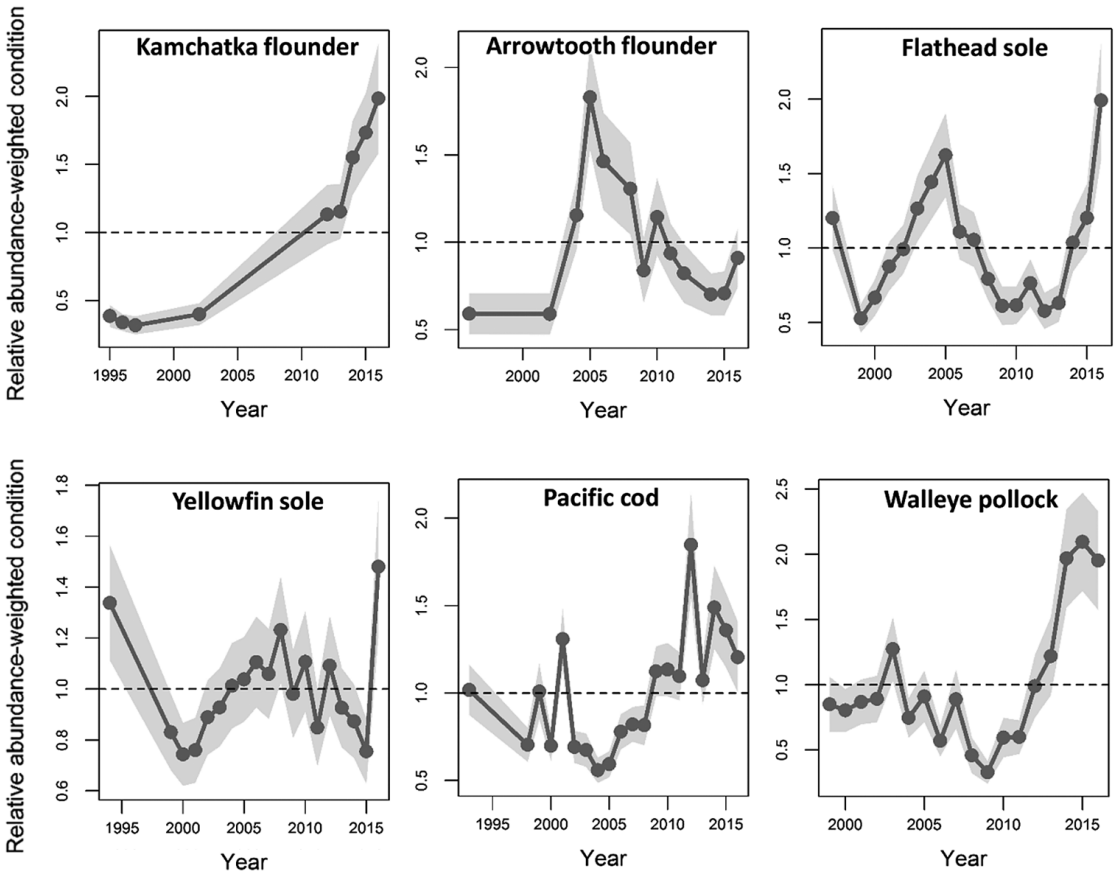

Fig. 7. Trends in relative abundance-weighted condition (grey line: mean; grey shading: 95% CI) predicted by the Akaike's information criterion-selected spatio-temporal models of the 6 study species. For each species, only predictions for those years where both density and length–weight data were available (Table 1) are shown. Relative abundance-weighted condition is abundance-weighted condition relative to mean abundance-weighted condition over the years for which both density and length–weight data were available

fish species (Kamchatka flounder, arrowtooth flounder, flathead sole, and yellowfin sole) was at or near its lowest level, and the abundance-weighted condition of Pacific cod and walleye pollock was also relatively low. In the very warm year of 2016 (the warmest year of the period 1992–2016; Fig. S1), the abundance-weighted condition of 4 of the 6 study species (Kamchatka flounder, flathead sole, yellowfin sole, and walleye pollock) was at or near its highest level, and the abundance-weighted condition of arrowtooth flounder and Pacific cod was also relatively high (Fig. 7).

4. DISCUSSION

Fish density can influence multiple life history processes, including natural mortality, growth, reproduction, and recruitment, with important consequences for resource management decisions (Stearns & Crandall 1984, Sánchez Lizaso et al. 2000, Forrest et al. 2013). However, modeling studies aiming to support resource management have generally only considered density-dependent effects on recruitment (Grüss et al. 2012, Andersen et al. 2017). Moreover, although there is growing research interest in measuring density dependence in growth (e.g. Lorenzen & Enberg 2002, Lorenzen 2016), this density dependence is generally not measured at fine spatial scales. In this study, we developed the first spatio-temporal statistical modeling approach simultaneously estimating changes in density and condition at fine spatial scales, which allows for the evaluation of the effects of density on fish condition. The application of our approach to 6 EBS groundfish species showed that condition and density are highly correlated for several species. Specifically, we found that (1) unmeasured variation in density that is stable over time (i.e. spatial variation in density) had a significant and strongly negative effect on unmeasured variation in

condition that is stable over time (i.e. spatial variation in condition) for 3 of the 4 study flatfishes, but a significant positive effect on spatial variation in condition for one gadoid (walleye pollock); and (2) unmeasured variation in density that changes between years (i.e. spatio-temporal variation in density) had a significant negative effect on unmeasured variation in condition that changes between years (i.e. spatio-temporal variation in condition) for one flatfish (arrowtooth flounder), and a significant positive effect on spatio-temporal variation in condition for one gadoid (Pacific cod).

We found that, in the EBS region, the influence of spatial variation in density on spatial variation in condition was more statistically significant than the influence of spatio-temporal variation in density on spatio-temporal variation in condition. We initially expected that spatio-temporal variation in condition would be more strongly impacted by changes in density than spatial variation in condition based on the results from Thorson (2015) for the California Current, one of the world's major upwelling systems. We suspect that our finding for the EBS is due to the fact that benthic production, which is more stable and lower over time than pelagic production, is more important in the EBS than in other marine regions like the California Current (McConnaughey & Smith 2000, Hunt et al. 2008). The importance of benthic production in the EBS may also be the reason why the influence of spatial variation in density on spatial variation in condition was found to be significant for the great majority of the studied benthic species (3 of the 4 flatfish species).

We also found that bottom temperature had large effects on both density and condition for the 6 studied species. First, the most parsimonious spatio-temporal model of all study species included bottom temperature effects on both density and condition. Then, the tendency for bottom temperatures to increase between the first (1992) and last year (2016) of the study period (Fig. S1) was accompanied by an overall increase in the abundance-weighted condition of 5 of the 6 species (Kamchatka flounder, arrowtooth flounder, flathead sole, Pacific cod, and walleye pollock) (Fig. 6). Finally, we found that the coldest and warmest years of the period 1992–2016 (1999 and 2016, respectively) were associated with, respectively, low and high fish condition for all study species, as shown previously by Boldt et al. (2015). Boldt et al. (2015) discussed that low fish conditions in the EBS in 1999 were likely due to the fact that low bottom temperatures reduced both prey productivity and predator–prey spatial overlap. Therefore, we conclude that forecasts of changes in weight-at-age within some EBS groundfish assessments will require an understanding of both density-dependence and bottom temperature effects on condition.

Local patterns of spatial and spatio-temporal variation in density and condition generally varied largely from one study species to another (Figs. 3, 5 & S4). Exceptions to this general pattern included Kamchatka flounder and arrowtooth flounder, whose patterns of spatial and spatio-temporal variation in density and condition were similar (Figs. 3, 4 & S4). This result is not surprising, as Kamchatka flounder and arrowtooth flounder share very similar biological and ecological attributes (Stevenson & Hoff 2009). However, while the local patterns of spatial and spatio-temporal variation in density and condition of Kamchatka flounder and arrowtooth flounder were similar, the abundance-weighted condition of the Kamchatka flounder population increased markedly over the period 1992–2016, while that of the arrowtooth flounder population increased until 2005 and tended to decrease afterwards. Interestingly, the abundance-weighted condition of the walleye pollock population followed opposite trends to that of the arrowtooth flounder population, namely decreasing until 2009 and then largely increasing. This result may stem from the fact that arrowtooth flounder is the major predator of walleye pollock (Hunsicker et al. 2013, Livingston et al. 2017). Thus, a reduction in arrowtooth flounder condition may decrease the level of predation pressure exerted by the arrowtooth flounder population on walleye pollock, which may allow walleye pollock to have longer foraging bouts and to grow larger, ultimately leading to an increase in walleye pollock condition. We also suspect that introducing arrowtooth flounder density as a covariate in the spatio-temporal model of walleye pollock may result in a more parsimonious and more reliable model.

Contrary to what was found for 3 of the study flatfishes (Kamchatka flounder, arrowtooth flounder, and yellowfin sole), spatial variation in walleye pollock density may have a significant positive effect on spatial variation in walleye pollock condition. The expected condition of walleye pollock is highest on the Outer Shelf of the EBS, where the expected density of the species is also generally high (Fig. 6a,b). This result may be due to the facts that bottom temperatures are stable on the Outer Shelf compared to the rest of the EBS and favorable to both walleye pollock density and condition (0–4°C in general; Table 3, Fig. S1), and that the abundance of many walleye pollock prey (fish prey, shrimps and, to a lesser

extent, Euphausiacea) is also high and conducive to better walleye pollock condition on the Outer Shelf (Livingston et al. 2017). We also found that, in warm years (e.g. 2016), walleye pollock condition becomes much higher on the Middle Shelf of the EBS (Figs. 6f & S4). This result concurs with previous studies that argued that the reduction of the cold pool in warm years allows groundfish species such as walleye pollock better foraging opportunities on the Middle Shelf of the EBS and, consequently, being in better condition (Hunt et al. 2008, Boldt et al. 2015).

As EBS bottom trawl surveys are conducted in June–July, we were able to investigate the potential for density-dependent changes in fish condition for the summer season only. However, most EBS groundfishes undertake large seasonal migrations (Witherell 2000, Boldt et al. 2015). For example, in winter, yellowfin sole are distributed on the Outer Shelf of the EBS and Pacific cod on the shelf edge and upper slope, and both species migrate to shallower waters in summer (Witherell 2000). Ideally, condition and density data should be collected by research surveys or fisheries observer programs outside of the summer season to understand how the seasonal migrations of EBS groundfishes affect their condition and relationships between density and condition.

For our application to EBS groundfish species, we employed total weights recorded during bottom trawl surveys rather than eviscerated weights to estimate fish condition. The liver of fishes is lightweight compared to their muscle mass (Lloret et al. 2014). Therefore, for fish species like small pelagics that store the bulk of their energy in muscles (Adams 1999), the use of total weights rather than eviscerated weights to estimate condition is not an issue. By contrast, in the case of most groundfishes, energy reserves are mainly stored in the liver (Lambert & Dutil 1997a). Thus, by employing total weights to estimate changes in groundfish condition, one may capture not only changes in physiological health and energetic status, but also other processes such as stomach fullness (Lloret et al. 2014, Brosset et al. 2015). Therefore, we encourage future studies applying our spatio-temporal model to groundfishes to use eviscerated weight data if those data are available in a reasonable amount.

We envision 3 avenues for future research in addition to the ones mentioned above. First, because the spatial distribution patterns of the juveniles and adults of most fish species are distinct, spatio-temporal models should ideally be developed separately for juveniles and adults for estimating simultaneous changes in condition and density. Second, one could conduct multi-species analyses using a more complex spatio-temporal model estimating spatial and spatio-temporal variation in density and condition for multiple species simultaneously (or for the juvenile and adult stages of multiple species simultaneously, if data availability allows) (Thorson & Barnett 2017). This more complex spatio-temporal model would employ a similar model structure (i.e. Eq. 6), but would associate each category c with a unique combination of species and variables (e.g. $c = 1$ and $c = 2$ would be density and condition for Kamchatka flounder, $c = 3$ and $c = 4$ would be density and condition for arrowtooth flounder, etc.). Multi-species analyses using the more complex spatio-temporal model would allow one to infer results for specific guilds (e.g. smallmouth versus predatory flatfishes), but also to estimate spatial and spatio-temporal variation in density and condition for species with few encounter data (which single-species spatio-temporal models are not able to do) (Thorson & Barnett 2017). Finally, in the present study, we considered only the effects of bottom temperatures on density and condition, but future studies may include more covariates in spatio-temporal models and evaluate which covariates have the strongest effects on density and condition (Thorson 2015). In this study, we allowed for linear and quadratic bottom temperature effects, but future studies could also consider spatially varying coefficients to explore non-local effects of oceanographic indices such as the cold pool (Thorson 2019b). Previous studies have shown that these oceanographic indices have a large impact on spatial distribution for demersal species in the EBS (Hunt et al. 2011, Hollowed et al. 2012), but they have not, to our knowledge, been applied in spatial models of fish condition.

In conclusion, our novel spatio-temporal modeling approach for simultaneously estimating changes in density and condition highlights the need to evaluate the impacts of accounting for or ignoring density-dependence and bottom temperature effects on condition within some EBS groundfish assessments (e.g. using a management strategy evaluation framework; Punt et al. 2016). We recommend that future studies use condition indices estimated with our approach to improve some EBS groundfish assessments (e.g. walleye pollock, arrowtooth flounder), by generating time-varying weight-at-age estimates (Thorson 2015), linking condition indices to natural mortality to produce more accurate natural-mortality-rates-at-age estimates (Casini et al. 2016), or relating reproductive potential to variation in the weight-at-length of fishes (Marshall & Frank 1999, Rideout et al. 2005, Jørgensen et al. 2006, Fitzhugh et al. 2012). We also rec-

ommend that future studies apply our approach to diverse marine ecosystems and to more species to better inform stock and habitat assessments (Marshall & Frank 1999, Lloret et al. 2002, Thorson 2015), as well as to answer important ecological questions such as the contribution of decreases in fish condition to marine population collapses (e.g. northern Gulf of St. Lawrence cod; Lambert & Dutil 1997b) or the impacts of density-dependent changes in condition on population biomasses and fisheries yields relative to those of density-dependent changes in recruitment (Andersen et al. 2017).

Acknowledgements. The present work was funded by the Habitat Information for Stock Assessments program (grant number 17-034). We are very grateful to Franz Mueter for his contribution to the proposal that funded this work, and to Tim Essington and Jodi Pirtle, as well as 3 anonymous reviewers, for insightful comments on earlier versions of the manuscript. The scientific results and conclusions, as well as any views or opinions expressed herein, are those of the authors and do not necessarily reflect those of NOAA or the US Department of Commerce.

LITERATURE CITED

Adams SM (1999) Ecological role of lipids in the health and success of fish populations. In: Arts MT, Wainman BC (eds) Lipids in freshwater ecosystems. Springer, New York, NY, p 132–160

Akaike H (1974) A new look at statistical-model identification. IEEE Trans Automat Contr 19:716–723

Andersen KH, Jacobsen NS, Jansen T, Beyer JE (2017) When in life does density dependence occur in fish populations? Fish Fish 18:656–667

Aydin K, Mueter F (2007) The Bering Sea — a dynamic food web perspective. Deep Sea Res II 54:2501–2525

Barrowman NJ, Myers RA (1996) Is fish recruitment related to spawner abundance? Fish Bull 94:707–724

Boldt JL, Haldorson LJ (2004) Size and condition of wild and hatchery pink salmon juveniles in Prince William Sound, Alaska. Trans Am Fish Soc 133:173–184

Boldt J, Rooper C, Hoff J (2015) Eastern Bering Sea groundfish condition. In: Zador S (ed) Ecosystem considerations 2015: status of Alaska's marine ecosystems. North Pacific Fishery Management Council, Anchorage, AK, p 182–190

Boxrucker J (1987) Largemouth bass influence on size structure of crappie populations in small Oklahoma impoundments. N Am J Fish Manage 7:273–278

Brosset P, Fromentin JM, Ménard F, Pernet F and others (2015) Measurement and analysis of small pelagic fish condition: a suitable method for rapid evaluation in the field. J Exp Mar Biol Ecol 462:90–97

Casini M, Bartolino V, Molinero JC, Kornilovs G (2010) Linking fisheries, trophic interactions and climate: threshold dynamics drive herring *Clupea harengus* growth in the central Baltic Sea. Mar Ecol Prog Ser 413:241–252

Casini M, Kornilovs G, Cardinale M, Möllmann C and others (2011) Spatial and temporal density dependence regulates the condition of central Baltic Sea clupeids: compelling evidence using an extensive international acoustic survey. Popul Ecol 53:511–523

Casini M, Rouyer T, Bartolino V, Larson N, Grygiel W (2014) Density-dependence in space and time: opposite synchronous variations in population distribution and body condition in the Baltic Sea sprat (*Sprattus sprattus*) over three decades. PLOS ONE 9:e92278

Casini M, Eero M, Carlshamre S, Lövgren J (2016) Using alternative biological information in stock assessment: condition-corrected natural mortality of Eastern Baltic cod. ICES J Mar Sci 73:2625–2631

Chambers RC, Leggett WC (1996) Maternal influences on variation in egg sizes in temperate marine fishes. Integr Comp Biol 36:180–196

Copeland T, Murphy BR, Ney JJ (2008) Interpretation of relative weight in three populations of wild bluegills: a cautionary tale. N Am J Fish Manage 28:368–377

Dutil JD, Godbout G, Blier PU, Groman D (2006) The effect of energetic condition on growth dynamics and health of Atlantic cod (*Gadus morhua*). J Appl Ichthyology 22: 138–144

Fitzhugh GR, Shertzer KW, Kellison GT, Wyanski DM (2012) Review of size- and age-dependence in batch spawning: implications for stock assessment of fish species exhibiting indeterminate fecundity. Fish Bull 110:413–425

Forrest RE, McAllister MK, Martell SJ, Walters CJ (2013) Modelling the effects of density-dependent mortality in juvenile red snapper caught as bycatch in Gulf of Mexico shrimp fisheries: implications for management. Fish Res 146:102–120

Francis R (1997) Comment: How should fisheries scientists and managers react to uncertainty about stock-recruit relationships? Can J Fish Aquat Sci 54:982–983

Froese R (2006) Cube law, condition factor and weight–length relationships: history, meta-analysis and recommendations. J Appl Ichthyology 22:241–253

Grüss A, Thorson JT (2019) Developing spatio-temporal models using multiple data types for evaluating population trends and habitat usage. ICES J Mar Sci 76:1748–1761

Grüss A, Kaplan DM, Lett C (2012) Estimating local settler–recruit relationship parameters for complex spatially explicit models. Fish Res 127-128:34–39

Grüss A, Biggs C, Heyman WD, Erisman B (2018) Prioritizing monitoring and conservation efforts for fish spawning aggregations in the US Gulf of Mexico. Sci Rep 8: 8473

Grüss A, Biggs CR, Heyman WD, Erisman B (2019a) Protecting juveniles, spawners or both: a practical statistical modelling approach for the design of marine protected areas. J Appl Ecol 56:2328–2339

Grüss A, Walter JF III, Babcock EA, Forrestal FC, Thorson JT, Lauretta MV, Schirripa MJ (2019b) Evaluation of the impacts of different treatments of spatio-temporal variation in catch-per-unit-effort standardization models. Fish Res 213:75–93

Hollowed AB, Barbeaux SJ, Cokelet ED, Farley E and others (2012) Effects of climate variations on pelagic ocean habitats and their role in structuring forage fish distributions in the Bering Sea. Deep Sea Res II 65-70:230–250

Hunsicker ME, Ciannelli L, Bailey KM, Zador S, Stige LC (2013) Climate and demography dictate the strength of predator-prey overlap in a subarctic marine ecosystem. PLOS ONE 8:e66025

Hunt GL, Stabeno PJ, Strom S, Napp JM (2008) Patterns of spatial and temporal variation in the marine ecosystem of

the southeastern Bering Sea, with special reference to the Pribilof Domain. Deep Sea Res II 55:1919–1944

Hunt GL, Coyle KO, Eisner LB, Farley EV and others (2011) Climate impacts on eastern Bering Sea foodwebs: a synthesis of new data and an assessment of the Oscillating Control Hypothesis. ICES J Mar Sci 68:1230–1243

Ianelli JN, Honkalehto T, Barbeaux S, Kotwicki S, Aydin K, Williamson N (2011) Assessment of the walleye pollock stock in the Eastern Bering Sea. In: Stock assessment and fishery evaluation report for the groundfish resources of the Bering Sea/Aleutian Islands regions. Alaska Fisheries Science Center, National Marine Fisheries Service, Seattle, WA, p 51–168

Ianelli JN, Honkalehto T, Barbeaux S, Kotwicki S (2014) Assessment of the walleye pollock stock in the Eastern Bering Sea. In: Stock Assessment and Fishery Evaluation Report for the Groundfish Resources of the Bering Sea/Aleutian Islands Regions. Alaska Fisheries Science Center, National Marine Fisheries Service, Anchorage, AK, p 55–156

Jørgensen C, Ernande B, Fiksen Ø, Dieckmann U (2006) The logic of skipped spawning in fish. Can J Fish Aquat Sci 63:200–211

Kass RE, Steffey D (1989) Approximate Bayesian inference in conditionally independent hierarchical models (parametric empirical Bayes models). J Am Stat Assoc 84:717–726

Kjesbu OS, Klungsøyr J, Kryvi H, Witthames PR, Walker MG (1991) Fecundity, atresia, and egg size of captive Atlantic cod (*Gadus morhua*) in relation to proximate body composition. Can J Fish Aquat Sci 48:2333–2343

Kjesbu OS, Kryvi H, Sundby S, Solemdal P (1992) Buoyancy variations in eggs of Atlantic cod (*Gadus morhua* L.) in relation to chorion thickness and egg size: theory and observations. J Fish Biol 41:581–599

Kristensen K, Nielsen A, Berg CW, Skaug H, Bell B (2016) TMB: automatic differentiation and Laplace approximation. J Stat Softw 70:1–20

Laman EA, Rooper CN, Turner K, Rooney S, Cooper DW, Zimmermann M (2018) Using species distribution models to describe essential fish habitat in Alaska. Can J Fish Aquat Sci 75:1230–1255

Lambert Y, Dutil JD (1997a) Can simple condition indices be used to monitor and quantify seasonal changes in the energy reserves of cod (*Gadus morhua*)? Can J Fish Aquat Sci 54:104–112

Lambert Y, Dutil JD (1997b) Condition and energy reserves of Atlantic cod (*Gadus morhua*) during the collapse of the northern Gulf of St. Lawrence stock. Can J Fish Aquat Sci 54:2388–2400

Laurel BJ, Spencer M, Iseri P, Copeman LA (2016) Temperature-dependent growth and behavior of juvenile Arctic cod (*Boreogadus saida*) and co-occurring North Pacific gadids. Polar Biol 39:1127–1135

Lauth RR, Conner J (2016) Results of the 2013 eastern Bering Sea continental shelf bottom trawl survey of groundfish and invertebrate resources. NOAA Tech Memo NMFS-AFSC-331

Le Cren ED (1958) Observation on the growth of perch (*Perca fluviatilis* L.) over twenty-two years with special reference to the effects of temperature and changes in population density. J Anim Ecol 27:287–334

Lindgren F (2012) Continuous domain spatial models in R-INLA. ISBA Bull 19:14–20

Lindgren F, Rue H (2015) Bayesian spatial modelling with R-INLA. J Stat Softw 63:1–25

Lindgren F, Rue H, Lindström J (2011) An explicit link between Gaussian fields and Gaussian Markov random fields: the stochastic partial differential equation approach. J R Stat Soc B 73:423–498

Livingston PA, Aydin K, Buckley TW, Lang GM, Yang MS, Miller BS (2017) Quantifying food web interactions in the North Pacific — a data-based approach. Environ Biol Fishes 100:443–470

Lloret J, Gil de Sola L, Souplet A, Galzin R (2002) Effects of large-scale habitat variability on condition of demersal exploited fish in the north-western Mediterranean. ICES J Mar Sci 59:1215–1227

Lloret J, Shulman G, Love RM (2014) Condition and health indicators of exploited marine fishes. Wiley-Blackwell, Oxford

Lo NC, Jacobson LD, Squire JL (1992) Indices of relative abundance from fish spotter data based on delta-lognormal models. Can J Fish Aquat Sci 49:2515–2526

Lorenzen K (2016) Toward a new paradigm for growth modeling in fisheries stock assessments: embracing plasticity and its consequences. Fish Res 180:4–22

Lorenzen K, Enberg K (2002) Density-dependent growth as a key mechanism in the regulation of fish populations: evidence from among-population comparisons. Proc R Soc B 269:49–54

Love RM (1958) Studies on the north sea cod. III. Effects of starvation. J Sci Food Agric 9:617–620

Marshall CT, Frank KT (1999) The effect of interannual variation in growth and condition on haddock recruitment. Can J Fish Aquat Sci 56:347–355

Marteinsdottir G, Steinarsson A (1998) Maternal influence on the size and viability of Iceland cod *Gadus morhua* eggs and larvae. J Fish Biol 52:1241–1258

McConnaughey RA, Smith KR (2000) Associations between flatfish abundance and surficial sediments in the eastern Bering Sea. Can J Fish Aquat Sci 57:2410–2419

Michalsen K, Ottersen G, Nakken O (1998) Growth of north-east Arctic cod (*Gadus morhua* L.) in relation to ambient temperature. ICES J Mar Sci 55:863–877

Murphy BR, Brown ML, Springer TA (1990) Evaluation of the relative weight (Wr) index, with new applications to walleye. N Am J Fish Manage 10:85–97

Nash RDM, Valencia AH, Geffen AJ (2006) The origin of Fulton's condition factor — setting the record straight. Fisheries (Bethesda, Md) 31:236–238

Pardoe H, Marteinsdóttir G (2009) Contrasting trends in two condition indices: bathymetric and spatial variation in autumn condition of Icelandic cod *Gadus morhua.* J Fish Biol 75:282–289

Pardoe H, Thórdarson G, Marteinsdóttir G (2008) Spatial and temporal trends in condition of Atlantic cod *Gadus morhua* on the Icelandic shelf. Mar Ecol Prog Ser 362: 261–277

Paul AJ, Paul JM (1999) Interannual and regional variations in body length, weight and energy content of age-0 Pacific herring from Prince William Sound, Alaska. J Fish Biol 54:996–1001

Punt AE, Butterworth DS, de Moor CL, De Oliveira JA, Haddon M (2016) Management strategy evaluation: best practices. Fish Fish 17:303–334

R Core Development Team (2019) R: a language and environment for statistical computing. R Foundation for Statistical Computing, Vienna

Rideout RM, Burton MPM, Rose GA (2000) Observations on mass atresia and skipped spawning in northern Atlantic

cod, from Smith Sound, Newfoundland. J Fish Biol 57: 1429–1440

Rideout RM, Rose GA, Burton MPM (2005) Skipped spawning in female iteroparous fishes. Fish Fish 6:50–72

Sánchez Lizaso J, Goñi R, Reñones O, Charton JG and others (2000) Density dependence in marine protected populations: a review. Environ Conserv 27:144–158

Shelton AO, Thorson JT, Ward EJ, Feist BE (2014) Spatial semiparametric models improve estimates of species abundance and distribution. Can J Fish Aquat Sci 71: 1655–1666

Stauffer G (2004) NOAA protocols for groundfish bottom trawl surveys of the nation's fishery resources. NOAA Tech Memo NMFS-F/SPO-65

Stearns SC, Crandall RE (1984) Plasticity for age and size at sexual maturity: a life-history response to unavoidable stress. In: Potts GW, Wooton RJ (eds) Fish reproductive strategies and tactics. Academic Press, New York, NY, p 13–30

Stevenson DE, Hoff GR (2009) Species identification confidence in the eastern Bering Sea shelf survey (1982-2008). AFSC Processed Report 2009-04. Alaska Fisheries Science Center, Seattle, WA

Thorson JT (2015) Spatio-temporal variation in fish condition is not consistently explained by density, temperature, or season for California Current groundfishes. Mar Ecol Prog Ser 526:101–112

Thorson JT (2018) Three problems with the conventional delta-model for biomass sampling data, and a computationally efficient alternative. Can J Fish Aquat Sci 75: 1369–1382

Thorson JT (2019a) Guidance for decisions using the Vector Autoregressive Spatio-Temporal (VAST) package in stock, ecosystem, habitat and climate assessments. Fish Res 210:143–161

Thorson JT (2019b) Measuring the impact of oceanographic indices on species distribution shifts: the spatially varying effect of cold-pool extent in the eastern Bering Sea. Limnol Oceanogr 64:2632–2645

Thorson JT (2019c) VAST model structure and user interface. https://github.com/James-Thorson-NOAA/VAST

Thorson JT, Barnett LA (2017) Comparing estimates of abundance trends and distribution shifts using single- and multispecies models of fishes and biogenic habitat. ICES J Mar Sci 74:1311–1321

Thorson JT, Shelton AO, Ward EJ, Skaug HJ (2015) Geostatistical delta-generalized linear mixed models improve precision for estimated abundance indices for West Coast groundfishes. ICES J Mar Sci 72:1297–1310

Thorson JT, Ianelli JN, Larsen EA, Ries L, Scheuerell MD, Szuwalski C, Zipkin EF (2016) Joint dynamic species distribution models: a tool for community ordination and spatio-temporal monitoring. Glob Ecol Biogeogr 25: 1144–1158

Wilkins NP (1967) Starvation of the herring, *Clupea harengus* L.: survival and some gross biochemical changes. Comp Biochem Physiol 23:503–518

Witherell D (2000) Groundfish of the Bering Sea and Aleutian Islands area: species profiles 2001, technical report. North Pacific Fishery Management Council, Anchorage, AK

Wuenschel MJ, McElroy WD, Oliveira K, McBride RS (2019) Measuring fish condition: an evaluation of new and old metrics for three species with contrasting life histories. Can J Fish Aquat Sci 76:886–903

Editorial responsibility: Stylianos Somarakis, Heraklion, Greece

Submitted: August 5, 2019; Accepted: December 4, 2019
Proofs received from author(s): January 27, 2020